J Intell Robot Syst (2014) 73:603–622
DOI 10.1007/s10846-013-9976-6

Fault-Tolerant Formation Driving Mechanism Designed for Heterogeneous MAVs-UGVs Groups

Martin Saska · Tomáš Krajník · Vojtěch Vonásek · Zdeněk Kasl · Vojtěch Spurný · Libor Přeučil

Received: 31 August 2013 / Accepted: 23 September 2013 / Published online: 12 October 2013

Abstract A fault-tolerant method for stabilization and navigation of 3D heterogeneous formations is proposed in this paper. The presented Model Predictive Control (MPC) based approach enables to deploy compact formations of closely cooperating autonomous aerial and ground robots in surveillance scenarios without the necessity of a precise external localization. Instead, the proposed method relies on a top-view visual relative localization provided by the micro aerial vehicles flying above the ground robots and on a simple yet stable visual based navigation using images from an onboard monocular camera. The MPC based schema together with a fault detection and recovery mechanism provide a robust solution applicable in complex environments with static and dynamic obstacles. The core of the proposed leader-follower based formation driving method consists in a representation of the entire 3D formation as a convex hull projected along a desired path that has to be followed by the group. Such an approach provides non-collision solution and respects requirements of the direct visibility between the team members. The uninterrupted visibility is crucial for the employed top-view localization and therefore for the stabilization of the group. The proposed formation driving method and the fault recovery mechanisms are verified by simulations and hardware experiments presented in the paper.

Keywords Mobile robots · Micro aerial vehicles · Formation driving · Fault detection and recovery · Model predictive control · Leader-follower · Trajectory planning

M. Saska (✉) · V. Vonásek · Z. Kasl · V. Spurný · L. Přeučil
Department of Cybernetics, Faculty of Electrical Engineering, Czech Technical University in Prague, Technicka 2, 166 27 Prague 6, Czech Republic
e-mail: saska@labe.felk.cvut.cz

V. Vonásek
e-mail: vonasek@labe.felk.cvut.cz

Z. Kasl
e-mail: kaslzden@fel.cvut.cz

V. Spurný
e-mail: spurnvoj@fel.cvut.cz

L. Přeučil
e-mail: preucil@labe.felk.cvut.cz

T. Krajník
Lincoln Centre for Autonomous Systems, Faculty of Science, University of Lincoln, Brayford Pool, Lincoln, LN6 7TS, Lincolnshire, UK
e-mail: tkrajnik@lincoln.ac.uk

1 Introduction

Integration of fault detection and recovery mechanisms into unmanned aerial systems is crucial

for improving their robustness and to enable their deployment in large closely cooperating teams. The identification of a sensor or actuator fault or even a failure of a team member makes possible to adapt the group behaviour, keeping the system operational with limited capabilities. This approach is especially appealing for formations and swarms of autonomous aerial, but also terrestrial vehicles, where the possibility of redundancy in robots' deployment is one of the key properties.

In this paper, a scenario of multi-robot surveillance is investigated. In the mission, a formation of autonomous vehicles has to repeatedly drive through a workspace in a phalanx to cover a large operating space. We propose to employ heterogeneous teams of autonomous micro-scale vertical take-off and landing vehicles (so called Micro Aerial Vehicles—MAVs) and Autonomous Ground Robots (UGVs). This allows us to consider their deployment in missions, which are impossible for solely MAVs or UGVs teams or in which these teams would not be efficient.

The MAVs can reach locations inaccessible by the UGVs. Beyond, they may provide a top view survey of the scene, which gives an important overview for human supervisors. On the contrary, the UGVs may operate in workspaces constrained by obstacles (e.g. in abundant vegetation). They can carry much heavier payload, which allows to use more powerful sensors. The UGVs have larger operational range and they may even provide an additional power source for the MAVs through a mobile heliport. These aspects attract us to take advantage of both platforms and to employ a heterogeneous MAVs-UGVs team. Besides, the co-existence of ground and flying robots can provide efficient solutions of fundamental formation driving problems, as is a precise and reliable relative localization of team members closely cooperating together. This approach reduces probability of collisions within the robotic group.

Usually, robots in reconnaissance and surveillance missions may not rely on pre-installed precise global localization infrastructures and commonly available systems (as GPS) lack required precision for control of compact formations. Besides, GPS lacks sufficient reliability mainly in urban and indoor environments. The proposed formation driving approach is suited for an onboard visual relative localization. The employed localization system uses simple light-weight cameras mounted on MAVs and identification patterns placed on UGVs and MAVs. The distance between the vehicles is then provided due to the known size of the patterns. Details on the visual based relative localization together with description of its precision and reliability is provided in [1]. With this top-view concept, one may better tackle the problem of loss of direct visibility that frequently occurs in the visual relative localization of ground robots operating in a workspace with obstacles. The possibility of team members' relative localization from above increases precision and reliability of the localization and brings another perspective to see the scene by operators supervising the mission.

Beyond the visual relative localization of individual robots, we propose to use a simple vision based technique also for the formation navigation in the environment. The presented formation driving method relies on a navigation approach called GeNav [2]. GeNav method uses features detected in images that are gathered by a monocular camera carried by a leader of the formation. This very simple method enables to robustly navigate the group along a pre-learnt path consisting of a sequence of straight segments (a proof of stability of this method can be found in [2]).

The combination of the top-view relative localization and the visual navigation provides a light-weight, low-cost, easy-to-deploy and efficient solution, which may act as an enabling technique for an extensive utilization of simple micro-scale robots. This paper is focussed on theoretical and technical aspects of the formation driving mechanism suited for the real-world deployment of autonomous robots under the GeNav navigation and the top-view localization, while technical details on the visual relative localization are available in [3] and the GeNav navigation in [2]. In addition, the paper addresses issues of the fault identification and recovery to increase robustness of the method. A mechanism to detect (and correct if possible) a malfunction of a single robot as well

as an inadvisable breakup of the group is proposed and experimentally verified.

2 State of the Art

The research endeavor in the formation driving community is aimed mainly at tasks of formation stabilization [4–6] and formation following a predefined path [7–10]. For example in [4], the task of formation stabilization and its convergence into a desired pattern is tackled for formations with communication delays. In [5], a multi-agent control system using artificial potential based on bell-shaped functions is proposed. The work in [6] employs a distributed iterative learning scheme for solving the formation control with switching strategy in the virtual structure and virtual leader-follower schemes.

The path following problem is tackled by designing a nonlinear formation control law based on the virtual structure approach via propagation of a virtual target along the path in [8]. In [7], the path following is investigated for groups of robots with limited sensing ranges. In [9], according to the leader-follower concept, the leader robot is forced to follow a given path, while the followers track the leaders's path with a fixed time delay. In [10], beyond the trajectory tracking, a possibility of an autonomous design of geometric pattern of the desired formation is discussed.

Beside the methods of the formation driving for UGVs, we should mention few approaches designed for UAVs [11–14]. In [11], the formation stabilization and keeping in the desired shape are treated as a dynamic 3D tracking problem, where the relative geometry of multiple UAVs is kept via a cascade-type guidance low under the leader-follower concept. A leader-follower approach for stabilization of helicopter's formations using a nonlinear model predictive control is proposed in [12] and optimized for on-line embedded solution enabling a response to the fast dynamic of UAVs in [13]. In [14], the formation stabilization of vertical take-off and landing unmanned aerial vehicles in presence of communication delays is addressed. Finally, let us mention work in [15] aimed at stabilization of a heterogeneous formation of UAVs above UGVs in circular orbits.

The above mentioned techniques are suited for utilization of robots under a precise external global localization system (for example approaches [13] are verified with the VICON system), for UGV formations they often rely on a dead reckoning with its cumulative error [8] or they provide theoretical solutions verified only by simulations [4, 5, 7, 9–12, 14], where a known position of robots may be assumed. In our work, the necessity of utilization of on-board systems for robots' localization and navigation is inherently included in the essence of the formation driving approach. The stabilization of the robot in the team is suited for requirements of available robust localization and navigation techniques, which enables its utilization in real-world scenarios.

The fault detection and recovery is an important and actual topic in the UAV (MAV) control nowadays due to the recent boom in the deployment of small unmanned vehicles. The fault detection techniques designed for a single vehicle can be divided into two categories: model–free and model–based. The model–free methods are based on analysis of the signal from sensors and do not rely on the model of the underlying system. As an example, let us mention an approach using neural networks to perform the signal analysis in order to acquire the information about a fault [16].

More frequently, methods for fault detection in unmanned aerial systems employ the model–based approach. They utilize residuals (difference between the sensor readings and expected values derived from a model of the monitored system) for the detection of occurrence of a fault. An example of an actuator fault diagnostic system designed for the nonlinear model of mini-quadrotors is available in [17]. Deployment of a methodology for actuator and sensor fault detection in an autonomous helicopter is presented in [18]. An autonomous actuator fault recovery mechanism based on an incorporation of a post-fault model of the actuator is proposed in [19]. This approach is extended for response to multiple actuator faults in [20].

Beyond the actuator faults in a single vehicle, this paper deals with the fault detection and recovery in the formation control. This problem is addressed for formations of terrestrial robots in [21]. In the paper, the formation is represented as a cellular automaton, where each formation member is represented as an individual cell, and the formation recovery is realized through a distributed auction–based mechanism. A fault tolerant approach designed for formations of quad–rotor UAVs is presented in [22]. The virtual structure based method is used for the formation trajectory planning, while the fault recovery is realized by a replanning to be able to response to a failure of a formation member. The most related work to the proposed paper is published in [23] and [24], where a vision–based relative position estimation for a team of UAVs is used in case of detection of fault in one of the onboard inertial systems. Although, the team of UAVs is not originally coordinated as a formation, a formation driving mechanism is employed in order to view the same scene from two UAVs (the faulty UAV and a faultless UAV used for its assistance) at the same time. Finally, let us mention two examples of the fault recovery in robotic swarms. In [25], an immune system reaction is employed. It solves the fault recovery problem through an isolation of the faulty robot from the swarm by neighbouring robots to protect the entire group. A fault detection method inspired by a light-based communication of fireflies, which spontaneously synchronize their rhythmic flashes, is presented in [26]. The method is based on analysing of anomalies from the synchronized light pulses of robots equipped with LEDs and light detectors.

Here, our contribution is an approach being able to detect faults in formation driving of heterogenous MAVs-UGVs groups stabilized under the top view localization. Beyond, we aim at re-coupling of inadvertently splitted formations caused by a fault in the system, but also by surrounding environment.

In our method, we rely on the Model Predictive Control (MPC) to be able to involve constraints imposed by the inter vehicle relations (shape of the formation feasible for the top-view relative localization), by vehicles (mobility constraints), by obstacles (environment constraints) and by the employed GeNav navigation of the entire group (straight line segments of the desired path) into the formation driving. The MPC approach is often used for stabilizing nonlinear systems with control constraints. In [12] and [13] it was shown, that the computational power of microprocessors available onboard of unmanned helicopters enables to employ MPC techniques also for the formation control of such a high dynamic systems, similarly as it is proposed here.

For descriptions and a general survey of MPC methods see [27–30] and references reported therein. In the formation driving, researchers take advantage of MPC mainly to respond to changes in dynamic environment [12, 13, 31–33]. In [31], authors introduce a new cost penalty in MPC optimization to guarantee a simple obstacle avoidance. Decentralized receding horizon motion planner introduced in [32] is developed for coordination of UGVs based on a motion planning independent to neighbors. The trajectory tracking mechanism developed in [33] is based on integration of a differential evolution algorithm into the MPC concept.

In our approach, we go beyond these papers in the following aspects. We apply the MPC method for the stabilization of the formation with included requirements of the top-view relative localization, which could be an enabling technique for deployment of heterogeneous MAVs-UGVs teams outside the laboratories. We present a novel obstacle avoidance function with a simple and effective representation of the 3D formation included. This approach provides a robust solution of the formation driving in environments with dynamic obstacles. Our formation driving method is designed for the purpose of simple yet stable visual navigation developed in [2], which is well suited for the reconnaissance and surveillance missions in environments without precise external localization. Beside the dynamic obstacles avoidance, the proposed method provides an inter-vehicle avoidance, which is crucial for failure tolerance of the system. All these behaviours and abilities are numerically and experimentally verified at the end of this paper.

This paper extends our previous work [34], where the basic formation driving mechanism based on the visual relative localization was

introduced. The main extension consists in the fault diagnosis and recovery mechanism that is introduced in Fig. 3 and described in details in Section 5. Beyond, results of new experiments and simulations verifying the proposed concept are published in Section 6.

3 Problem Statement and Preliminaries

Development of method presented in this paper is motivated by reconnaissance applications, where a team of robots has to autonomously follow a desired path given by a supervising expert. During the movement along the path, the robots have to keep a formation suited for the mission requirements. The robots can form a searching phalanx (a line formation) to be able to search for victims or intruders in large areas or a compact fleet of vehicles can be used for transportation purposes. We assume that one robot of the group (UGV or MAV), called GeNav leader in this paper, is capable of autonomous navigation along such a path. We will employ a navigation system based on detection of SURF features in an image provided by an on-board camera. The system was developed for navigation of a single UGV robot [2] and later extended for a quadrocopter [35]. This system (called as GeNav) is suited for guidance of robots along path that consists of a sequence of straight segments. Its precision (∼20 cm) and reliability enables a robust navigation of a single robot, but it is not sufficient for the coordination of the robots within a compact formation with small relative distances between robots.

Beside the GeNav leader, we assume to use a group of simple UGV followers without any on-board sensors for their localization and a group of MAV followers (quadrotors) equipped with a bottom camera and a system for visual relative localization [3]. This system provides information on the relative position between the camera of MAVs and center of an identification pattern. The identification patterns are carried by all UGVs and MAVs except the one flying in the highest altitude. The precision of the employed visual relative localization system (∼1 cm) is sufficient for the formation stabilization in the desired shape. We assume that the shape is designed to satisfy the condition that all robots, except the MAV flying in the highest altitude, are in the field of view of at least one bottom camera mounted on an MAV.

Now, let us describe preliminaries important for description of the method, in which the heterogeneous 3D formation of MAVs and UGVs has to follow the desired path, while requirements of the formation driving and the top-view relative localization are satisfied. It means that (1) the movement of the formation has to be smooth also in the unsmooth connections of straight path segments, where the GeNav leader is turning around on the spot, and (2) the direct visibility between the vehicles have to be kept during the formation deployment.

Let $\psi_j(t) = \{x_j(t), y_j(t), z_j(t), \varphi_j(t)\}$, where $j \in \{GL, VL, 1, \ldots, nf\}$, denote configurations of the GeNav leader GL, a virtual leader VL, and nf followers at time t. The GeNav leader is equipped with the on-board visual navigation to follow the pre-learnt path segments. It is positioned in front of the formation and it is used as a reference point for the coordinate system used by the top-view relative localization. Whereas, the virtual leader is a reference point for the proposed formation driving technique. Virtual leader is initially placed in the same position and orientation as the GeNav leader. Using the trajectory following approach described in Section 4.3, it keeps the same position as GeNav leader except the deviation caused by obstacles that could break the top view localization or to cause collisions. Significant deviation of GL and VL positions can be also seen in connections of line segments of the desired path. In these points, the path is not feasible for the formation of nonholonomic robots, which forces the virtual leader to temporarly leave the path to be able to follow a smooth trajectory feasible for the formation.

The Cartesian coordinates $x_j(t)$, $y_j(t)$ and $z_j(t)$ define positions $\bar{p}_j(t)$ of all robots (leaders and followers) and $\varphi_j(t)$ denotes their heading. Both MAVs and UGVs (except the robot assigned as the GeNav leader) are denoted as followers in the presented approach. For the MAVs, the heading $\varphi_j(t)$ becomes directly the yaw (see Fig. 1 for the coordinate system of MAVs). Roll together with pitch do not need to be included in the kinematic model employed in MPC, but they depend on the

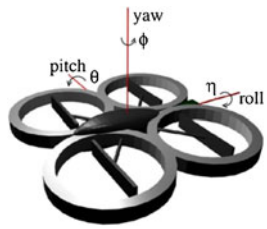

Fig. 1 MAV coordinate system

type of utilized MAVs as shown for a quadrotor in [36].

Let us assume that the environment contains a finite number n_0 of compact obstacles. The obstacles can be static (as part of a known map) or dynamic and unknown (detected during the formation movement by on-board sensors). These updates of the map are shared by all robots via a Wi-Fi communication. A follower or even more followers of the formation can become dynamic obstacles if deviating from their desired positions as demonstrated in the failure tolerance simulation in Section 6.

The kinematics for any robot j in 3D is described by the simple nonholonomic kinematic model: $\dot{x}_j(t) = v_j(t)\cos\varphi_j(t)$, $\dot{y}_j(t) = v_j(t)\sin\varphi_j(t)$, $\dot{z}_j(t) = w_j$ and $\dot{\varphi}_j(t) = K_j(t)v_j(t)$, where feed-forward velocity $v_j(t)$, curvature $K_j(t)$ and ascent velocity $w_j(t)$ represent control inputs denoted as $\bar{u}_j(t) = \{v_j(t), K_j(t), w_j(t)\}$. We assume that UGVs operate in a flat surface and that $z_j(\cdot) = 0$ and $w_j(\cdot) = 0$ for each of the UGVs. In case of MAVs, $v_j(\cdot)$, $K_j(\cdot)$ and $w_j(\cdot)$ values are inputs for the low level controller, as shown in [36].

Let us now describe a discretization of the kinematic model as it is used in the proposed formation driving with the model predictive trajectory following included. Let us define a time interval $[t_0, t_{\text{end}}]$ consisting of a sequence of elements of increasing times $\{t_0, t_1, \ldots, t_{\text{end}-1}, t_{\text{end}}\}$, such that $t_0 < t_1 < \ldots < t_{\text{end}-1} < t_{\text{end}}$. We will refer to t_k using its index k in this paper. For the model predictive planning, the control inputs are held constant over each time interval $[t_k, t_{k+1})$, where $k \in \{0, \ldots, end\}$. We will call the points at which the control inputs change as *transition points*. By integrating the kinematic model over these intervals, the following discretized model may be obtained:

if $K_j(k+1) \neq 0$:

$$
\begin{aligned}
x_j(k+1) &= x_j(k) + \frac{1}{K_j(k+1)} \\
&\quad \times \left[-\sin\left(\varphi_j(k)\right) + \sin\left(\varphi_j(k)\right.\right. \\
&\quad \left.\left. + K_j(k+1)v_j(k+1)\Delta t\right)\right], \\
y_j(k+1) &= y_j(k) - \frac{1}{K_j(k+1)} \\
&\quad \times \left[-\cos\left(\varphi_j(k)\right) + \cos\left(\varphi_j(k)\right.\right. \\
&\quad \left.\left. + K_j(k+1)v_j(k+1)\Delta t\right)\right], \\
z_j(k+1) &= z_j(k) + w_j(k+1)\Delta t \\
\varphi_j(k+1) &= \varphi_j(k) + K_j(k+1)v_j(k+1)\Delta t
\end{aligned}
$$

and if $K_j(k+1) = 0$:

$$
\begin{aligned}
x_j(k+1) &= x_j(k) + v_j(k+1)\cos\left(\varphi_j(k)\right)\Delta t, \\
y_j(k+1) &= y_j(k) + v_j(k+1)\sin\left(\varphi_j(k)\right)\Delta t, \\
z_j(k+1) &= z_j(k) + w_j(k+1)\Delta t \\
\varphi_j(k+1) &= \varphi_j(k), \qquad (1)
\end{aligned}
$$

where $x_j(k)$, $y_j(k)$ and $z_j(k)$ are the rectangular coordinates and $\varphi_j(k)$ the heading angle at the transition point with index k. Δt is a sampling time, which is uniform in the whole interval $[t_0, t_{\text{end}}]$. The control inputs $v_j(k+1)$, $K_j(k+1)$ and $w_j(k+1)$ are constant between transition points with index k and $k+1$.

As mentioned in the problem statement, we assume a heterogeneous 3D formation of a given shape, which satisfies the requirements given by the formation driving and the top-view localization: (1) robots are in a safe relative distance; (2) each robot, except the MAV flying in the highest altitude, is observed by at least one MAV. In this paper, the shape of the entire formation is maintained with a leader-follower technique derived from the approach [37], which was designed for formations of UGVs working in a planar

environment. For the heterogeneous MAVs-UGVs formations, we have extended the notation from [37] to 3D as visualized in Fig. 2. Besides, we have extended the technique in [37], which is designed for following smooth splines (continuity of second-order is required), for utilization of paths consisting of straight line segments, which are required by the GeNav navigation.

In our method, both types of followers, MAVs and UGVs, follow the trajectory of the virtual leader in distances defined in p, q, h curvilinear coordinate system. The position of each follower i is uniquely determined by states $\psi_{VL}(t_{p_i})$ in *travelled distance* p_i from the actual position of the virtual leader along the virtual leader's trajectory, by *offset distance* q_i from the trajectory in perpendicular direction and by elevation h_i above the trajectory. t_{p_i} is the time when the virtual leader was at the *travelled distance* p_i behind its actual position. To get states of follower i in rectangular coordinates, states of the virtual leader at time t_{p_i}, which is $\psi_{VL}(t_{p_i}) = \{x_{VL}(t_{p_i}), y_{VL}(t_{p_i}), z_{VL}(t_{p_i}), \varphi_{VL}(t_{p_i})\}$, have to be shifted with vector $V(t_{p_i})$ as follows:

$$\psi_i(t) = \psi_{VL}(t_{p_i}) + V(t_{p_i}). \tag{2}$$

The vector $V(t_{p_i})$ consists of four components: $V(t_{p_i}) = (-q_i \sin(\varphi_L(t_{p_i})), q_i \cos(\varphi_L(t_{p_i})), h_i, 0)$.

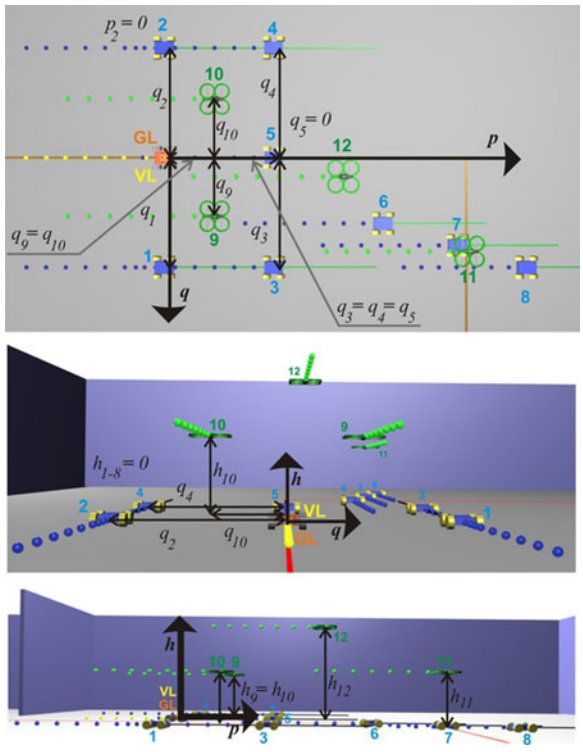

Fig. 2 The desired shape of the formation described in curvilinear coordinates

4 Integrated Trajectory Planning and Formation Stabilization

4.1 Method Overview

The system designed for the stabilization of heterogeneous MAVs-UGVs formations is divided into four main blocks as you can see in the scheme depicted in Fig. 3. The first block, *GeNav Leader*, is responsible for navigation of the entire formation in the environment. It provides control inputs for the GeNav leader based on image features gained by an onboard camera. The GeNav method enables to navigate a robot or a group of robots along a pre-learnt path consisting of straight segments. The requirements on the piecewise straight desired path is important for stability of the method as analysed in [2].

From the formation stabilization perspective, an important output of the *GeNav Leader* module is a prediction of GeNav leader's states. For the prediction, it is assumed that the GeNav leader follows the desired path without any perturbation in both, the desired speed and the position on the path. The perturbations, which occur in real robotic systems, will be diminished by the presented receding horizon control technique. The predicted trajectory, which consists of n states derived with constant sampling time Δt, acts as an input of the *Virtual Leader* block.

This part is important for avoidance of obstacles that could affect the relative localization within the group or that could collide with robots of the formation. Besides, it enables to follow the GeNav leader in connections of straight line segments of the desired path. In the *Virtual*

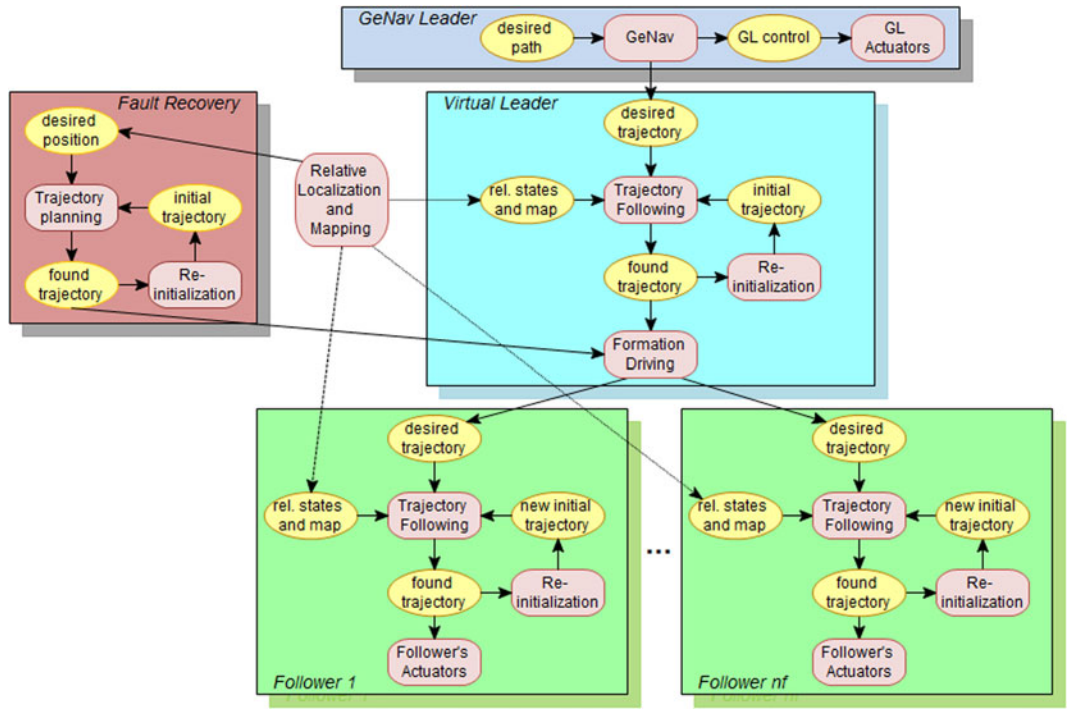

Fig. 3 Schema of the complete planning and control system

Leader part, the *Trajectory Following* block provides control inputs for the virtual leader, which are feasible for the entire formation and respect the requirements of the top-view relative localization via the model of the formation. In the straight segments of the desired path, the trajectory found by the *Trajectory Following* block follows the desired trajectory with minimal deviation and it is only employed to diminish possible perturbations. A significant difference between the desired and found trajectory occurs mainly due to appearing obstacles or near to line segment connections. Details on the trajectory following mechanism with emphasis on incorporation of the 3D heterogeneous formation stabilized under the top-view localization are presented in Section 4.3.

The resulting trajectory obtained in the *Trajectory Following* block is described by a sequence of configurations of the virtual leader $\psi_L(k)$, where $k \in \{1, \ldots, N\}$, and by constant control inputs applied in between the transition points. According the MPC concept, only a portion of the computed control actions is applied on the interval $\langle t_0, t_0 + n\Delta t\rangle$, known as the receding step. This process is then repeated on the interval $\langle t_0 + n\Delta t, t_0 + N\Delta t + n\Delta t\rangle$ as the finite horizon moves by *time steps* $n\Delta t$, yielding a state feedback control scheme strategy. The unused part of the trajectory can be employed for re-initialization of the planning process in each planning step, since the plan of the formation between two consequent steps is usually changed only slightly. To summarize this, n is number of transition points in the part of the planning horizon, which is realized by robots in each planning step, and N is the total number of transition points in the planning horizon.

In the proposed formation driving system, the trajectory obtained in the *Trajectory Planning* block is used as an input for the *Formation Driving* module, which transforms the plan to desired configurations of followers (using Eq. 2). The core of the third main block, which is multiplied for MAVs and UGVs followers, is also

the *Trajectory Following* module. This part is responsible for avoiding of impending collisions with obstacles or other members of the team and it corrects deviations from the desired trajectory provided by the virtual leader. In real applications with dynamic obstacles and disturbances caused by the imprecise model of sensors and actuators, the desired trajectories provided by the *Formation Driving* cannot be directly applied for control of particular followers. They have to be adapted to ensure the stability of the group and non-collision movement. Similarly as in the leader's trajectory following, the unused part of the found trajectory can be employed for the initialization of the planning process.

The fourth main block, labelled as *Fault Recovery*, is employed only if an unwished splitting of the formation is detected. In such a case, a new virtual leader is created to lead the unstuck part of the former group. Its aim is to navigate the sub-group back to its desired position within the main formation. It uses the extended MPC trajectory planning approach described in details in Section 5.2.

A communication (via WiFi) is required only between the GeNav leader and particular followers. It is assumed that the *GL* and *VL* modules are realized on the same vehicle. Also the data from the relative localisation processes are stored there. Therefore, the communication between the GeNav leader and followers is limited to sending the desired trajectory and actual data from the visual relative localization.

Finally, let us remark that the trajectories of virtual leader and followers are given in the local frame of the GeNav leader, since all members of the formation know its relative position provided by the top-view localization.

4.2 3D Formation Representation for the Obstacle Avoidance

One of the main contribution of this work is the ability of the system to ensure formation stabilization under the top-view visual relative localization in environments with dynamic obstacles. This requires to design an obstacle avoidance function included into the trajectory following method, which is introduced in Fig. 3. The core of the avoidance function is a proper representation of the entire formation, which incorporates the requirement on the direct visibility between the robots into the formation stabilization process.

In our approach, the 3D formation is represented by a convex hull of positions of followers projected into a plane $\mathcal{P}_{VL}$, which is orthogonal to the trajectory of the virtual leader in its actual position (see Fig. 4). The projection of the position of i-th follower into the plane $\mathcal{P}_{VL}$ can be simply obtained as $x_i^{VL} := q_i$ and $y_i^{VL} := h_i$, where $\{x^{VL}; y^{VL}\}$ is coordinate system in the plane $\mathcal{P}_{VL}$ as sketched in Fig. 4. The convex hull of the set of points $\{x_i^{VL}; y_i^{VL}\}$, where $i \in \{1, \ldots, nf\}$, is an appropriate representation of the 3D formation under the top-view relative localization by two reasons: (1) Each follower i intersects the plane $\mathcal{P}_{VL}$ at point $\{x_i^{VL}; y_i^{VL}\}$ in future. (2) The convex hull of such a set of points denotes borders of the area, which should stay obstacle free. This ensures that the direct visibility between MAVs and UGVs, which is crucial for the presented top-view visual localization, is satisfied.

Moreover for the obstacle avoidance function presented in Section 4.3, the convex hull (CH) needs to be dilated by a detection boundary radius r_s to keep obstacles in a desired distance from followers. Only obstacles that are closer to the convex hull than r_s are considered in the avoidance

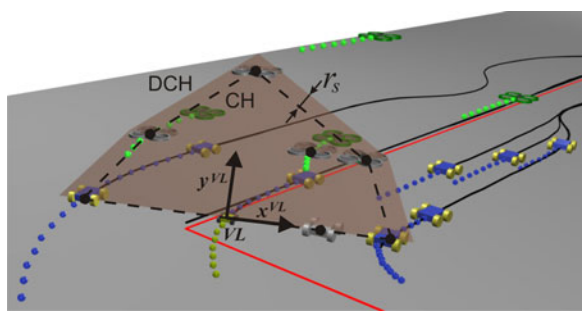

Fig. 4 *Dilated convex hull*. The *shaded contours with black balls* represent projections of followers into the plane of virtual leader

function. In the trajectory following process applied for control of followers, the DCH is reduced to a circle with radius equal to r_s to represent a single robot.

4.3 Trajectory Planning and Control Mechanism

Let us now describe the trajectory following mechanism with obstacle avoidance function more in details. As mentioned above, the aim of the method is to find a control sequence that steers the virtual leader along the desired path followed by the GeNav leader and consequently to find control sequences that stabilize the followers behind the virtual leader in desired relative positions. The intention of the method is to find such control sequences that keep the virtual leader as close as possible to the GeNav leader and followers as close as possible to their desired position behind the virtual leader, while satisfying the requirements given by the non-collision formation driving and the top-view relative localization. By applying this concept, the group is able to respond to changes in workspace, which can be dynamic or newly detected static obstacles, and to failures of a robot of the team.

To define the trajectory planning problem in a compact form, we need to gather states $\psi_j(k)$, where $k \in \{1, \ldots, N\}$ and $j \in \{VL, 1, \ldots, n_r\}$, into vector $\Psi_j \in \mathbb{R}^{4N}$ and control inputs $\bar{u}_j(k)$ into vector $\mathcal{U}_j \in \mathbb{R}^{3N}$. Then all variables describing the trajectory of the virtual leader or a follower can be collected in an optimization vector: $\Omega_j = [\Psi_j, \mathcal{U}_j] \in \mathbb{R}^{7N}$. Let us now transform the trajectory planning to minimization of a cost function $J_j(\Omega_j)$, $j \in \{VL, 1, \ldots, n_r\}$, subject to sets of equality constraints $h_j(k) = 0$, $\forall k \in \{0, \ldots, N-1\}$, and inequality constraints $g_j(k) \leq 0$, $\forall k \in \{1, \ldots, N\}$. The proposed cost function consists of four components:

$$
\begin{aligned}
J_j(\Omega_j) = & \sum_{k=1}^{N} \left\| \left(\bar{p}_{d,j}(k) - \bar{p}_j(k) \right) \right\|^2 \\
& + \sum_{l=1}^{n_o} \left(\min \left\{ 0, \frac{d_{DCH}(\Omega_j, o_l)}{d_{DCH}(\Omega_j, o_l) - R_{DCH}} \right\} \right)^2 \\
& + \frac{1}{N} \sum_{k=1}^{N} \left(v_j(k) - \bar{v}_j \right)^2 + \left(K_j(k) - \bar{K}_j \right)^2 \\
& + \sum_{f \in \bar{n}_n} \left(\min \left\{ 0, \frac{d_{j,f}(\Omega_j, \Omega_f^\circ) - r_{s,j}}{d_{j,f}(\Omega_j, \Omega_f^\circ) - r_{a,j}} \right\} \right)^2 .
\end{aligned}
\tag{3}
$$

The first part penalizes solutions with states deviated from the desired states $\bar{p}_{d,j}(k)$, where $k \in \{1, \ldots, N\}$. In the virtual leader's trajectory tracking, the desired states are obtained by the prediction of the movement of the GeNav leader. In the followers' trajectory planning, the desired states are derived from the result of the virtual leader's trajectory tracking using the formation driving concept for each of the followers.

The second term of $J_j(\Omega_j)$ contributes to the final cost when an obstacle is inside the projection of the dilated convex hull along the planned trajectory. As mentioned, the convex hull represents the formation in case of the virtual leader's trajectory planning or a single robot in case of the followers' trajectory planning. Examples of the projected convex hull are shown in Fig. 5. The value of the second term of $J_j(\Omega_j)$ will be increasing

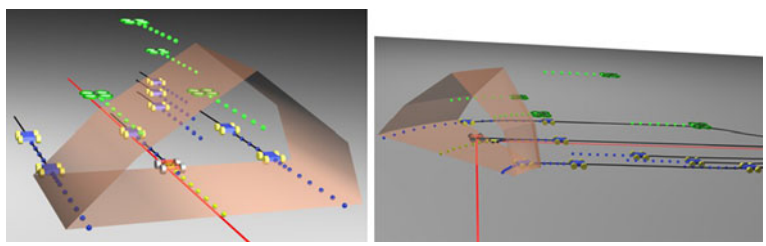

(a) Formation in a straight segment of the path.

(b) Formation in a connection of line segments.

Fig. 5 The *dilated convex hull* projected along the planned trajectory of the virtual leader

as the obstacle is approaching to the centre of the convex hull. The constant R_{DCH} is equal to half of the maximal width of the dilated complex hull measured in the x^L coordinate ($R_{DCH} = r_s$ in the followers' trajectory planning). The function $d_{DCH}(\Omega_j, o_l)$ provides distance from the dilated convex hull to obstacle o_l again in the direction of x^L coordinate. The function value is negative if the obstacle is outside the dilated convex hull and positive if the obstacle is in the hull. The direction of the gradient of such defined avoidance function is to the side of the hull in the x^L coordinate. This is important since the formation, which is "fixed" by UGVs to the ground, cannot avoid obstacles by change of its altitude.

The third term is important for the reducing of undesirable oscillations in movement of robots and it eliminates needless aggressive manoeuvres. This term penalises high variance of control inputs. During the optimization process, solutions with control inputs deviating from their mean values, $\bar{v}_j = \frac{1}{N}\sum_{k=1}^{N} v_j(k)$ and $\bar{K}_j = \frac{1}{N}\sum_{k=1}^{N} K_j(k)$, are penalized, which results into smooth trajectories.

Finally, the last part of the cost function $J_j(\Omega_j)$ is crucial for the failure tolerance of the system. This term is a sum of avoidance functions in which the other members of the team are considered also as dynamic obstacles. This part has to protect the robots in case of an unexpected behaviour of a defective neighbour. Function $d_{j,f}(\Omega_j, \Omega_f^\circ)$ provides minimal distance between the planned trajectory Ω_j of $j-th$ follower and the recent plan Ω_f° of f-the robot. The $(\cdot)^\circ$ symbol denotes the last results of the optimization process for the particular robot. The minimal distance is provided for all $f \in \bar{n}_n$, where $\bar{n}_n = \{1, \ldots, j-1, j+1, \ldots, n_r\}$. The detection radius $r_{s,j}$ is usually smaller than the basic detection radius r_s used for the dilation of the convex hull, because the follower should not try to avoid a close neighbour if both are at the desired position. Beside the detection radius, we need to define a circular avoidance boundary with radius $r_{a,j}$, where $r_{s,j} > r_{a,j}$. While, single robots should not respond to other followers detected outside the region with radius $r_{s,j}$, distance between the robots and their neighbours less than $r_{a,j}$ is considered as inadmissible (it could cause a collision).

The equality constraints $h(k)$ represent the kinematic model (1) for all $k \in \{0, \ldots, N-1\}$ with initial conditions given by the actual state of the leader. This ensures that the obtained trajectory stays feasible with respect to kinematics of utilized robots. It means that these constraints are satisfied if $\psi_j(k+1)$ is obtained by substituting the vectors $\psi_j(k)$ and $\bar{u}_j(k+1)$ into the Eq. 1 for all $k \in \{0, \ldots, N-1\}$.

The sets of inequality constraints $g(k)$ characterize bounds on control inputs $\bar{u}_j(k)$ for all $k \in \{1, \ldots, N\}$. For all followers, the control inputs are limited by vehicle mechanical capabilities (i.e., chassis and engine) as $v_{\min,i} \le v_i(k) \le v_{\max,i}$, $|K_i(k)| \le K_{\max,i}$ and for MAVs also $w_{\min,j} \le w_j(k) \le w_{\max,j}$. These values may differ for each of the followers. For the virtual leader, these limits have to be extended, since the constraints of the entire formation need to be included. The trajectory of the virtual leader must be feasible for all followers in their desired positions. For the virtual leader, the admissible control set can be determined using the leader-follower approach as $\max_{i=1,\ldots,n_r}\left(\frac{-K_{\max,i}}{1-q_i K_{\max,i}}\right) \le K_{VL}(k) \le \min_{i=1,\ldots,n_r}\left(\frac{K_{\max,i}}{1+q_i K_{\max,i}}\right)$ and $\max_{i=1,\ldots,n_r}\left(\frac{v_{\min,i}}{1+q_i K_L(t)}\right) \le v_{VL}(k) \le \min_{i=1,\ldots,n_r}\left(\frac{v_{\max,i}}{1+q_i K_L(t)}\right)$. These restrictions must be applied to respect different values of curvature and speed of robots in different positions within the guided formation. Intuitively, e.g. the robot following the inner track during a turning movement goes slower but with a bigger curvature than the robot further from the center of the turning.

5 Fault Diagnosis and Recovery in Formation Control

Faults in multi-robot systems and especially in formations or swarms of various aerial, ground, water, or underwater robots can be investigated in several levels of abstraction. In the most general case, the compact group as a whole can fail in carrying out its task or mission. The second case of faults in multi-robot applications represents examples, where the group is able to continue with performing its task in a limited way, e.g. a

robot or even several robots (a sub-group) from the original group is lost. Finally, we should mention the situation in which all robots can continue towards fulfilment their task, but some of them in a limited way. This case is referred as component/components failure of a robot, where the component may be either a sensor or an actuator.

Similarly, the following faults can occur in the proposed approach of heterogeneous 3D formation driving due to numerous reasons.

(1) The entire formation can fail if the GeNav leader loses its path to follow.
(2) The compact formation is not able to follow the GeNav leader, e.g. due to the motion constraints or constraints given by surrounding environment.
(3) An undesirable separation of a follower or a sub-group of followers from the main formation can be caused by several reasons: lost of the relative localization, influences of the environment or serious failure of robot's motion abilities to name few.
(4) Finally, a fault of a robot's component, which influences its ability to follow the formation, may occur in both, MAV and UGV platforms.

The performance and stability of the GeNav technique, which is employed by the GeNav leader, is investigated and sufficiently described in [2] and therefore the first item of the list will be skipped in the following analyses. In case of a component failure (the last item of the list), which may be a malfunction of a sensor or actuator that is not fatal for the ability to follow the group, the MPC correction mechanism in the replanning loop takes place. Even in a case of strong disturbances, which significantly change the system in comparison with the model applied in the predictive control, the deviation from the desired position is continuously corrected due to the periodical replanning. If the disturbances exceed a tolerable limit and the MPC mechanism is not able to stabilize the robot within the formation, the situation may be considered as the undesirable separation of a follower (the second item of the list).

Therefore, only two points have to be resolved to fully analyse the behaviour of the presented formation driving mechanism and to enable recovery in case of failures.

- Fault–detection and recovery of the virtual leader's trajectory tracking mechanism (the second item of the list).
- Fault–detection and recovery of the followers' trajectory tracking mechanism (the third item of the list).

Remaining types of faults, which do not lead to the separation of a robot/robots from the formation, can be compensated by the MPC replanning as it is usual.

5.1 Failure Detection

Failures of the virtual leader's as well as followers' trajectory tracking mechanisms can be detected simply by observing the progress of values of function (3) since the same optimization function is used for solving both problems. The deviation of the system (virtual leader or a follower) from its desired position is penalized only by the first term of function (3). The functional value of this term corresponds not only to the actual deviation of the system, but it characterizes also its progress in future. Therefore, an increase of this value in a longer time period indicates that the stabilization mechanism is not able to compensate the deviation. The particular system (a follower or the virtual leader) can be considered as a lost entity and a recovery mechanism has to be activated. It is worth to mention that the value of the first term of Eq. 3 can be temporary increased also due to an obstacle avoidance manoeuvre. Therefore, the threshold signalising the separation of the controlled system has to be higher than the peaks caused by obstacles or a reasoning mechanism with included information given in the second and fourth terms of Eq. 3, where the obstacle proximity is penalized, has to be employed. In the presented experiments, a threshold exceeding the peaks of the value of the first term in Eq. 3, which are caused by the obstacles, has been used with sufficient reliability. Exceeding of this threshold then indicates the formation decay and it is not caused by the regular obstacle avoidance. Once the splitting of the formation or the malfunction of

the virtual leader is detected, the failure recovery mechanisms introduced in Fig. 3 and described in details in the following paragraph needs to be run.

5.2 Fault-Tolerant Formation Control

The purpose of this section is not to present the well known MPC technique being able to compensate partial faults and uncertainties of sensors and actuators, but to describe the novel mechanism developed to recovery the splitted formation. The proposed approach is based on creating an ad-hoc virtual leader for commanding the unstuck group back to its desired position (referred to as DP) within the former formation. To be accurate, we should clarify that the desired position DP corresponds to the desired position of the virtual leader that leads the new formation.

The standard MPC scheme with the limited control horizon with a constant sampling time Δt in-between of N transition points may not be sufficient for the navigation of the unstuck part of the formation back to its position if the distance to the rest of the group significantly exceeds the length of the horizon. A simple prolonging of the horizon would quickly touch the limits of available computational resources. Therefore, we propose to extend the control scheme of the virtual leader with an additional planning horizon with variable sampling time in-between of transition points. This horizon is used for the trajectory planning of the separated formation/robot into its desired position DP. The entire horizon is then divided into two segments, the standard control horizon and the planning horizon. In the planning horizon, lengths of time intervals between transition points are also variables taking part in the planning problem. This planning algorithm again respects constraints given by the top view localization and by kinematics of followers to be sure that the plan is feasible in case of a sub-formation breakaway.

To define the trajectory planning problem with two time intervals in a compact form we need to gather states $\psi_j(k)$, where $k \in \{N+1, \ldots, N+M\}$, and control inputs $\bar{u}_j(k)$, where $k \in \{N+1, \ldots, N+M\}$, into vectors $\Psi_{j,M} \in \mathbb{R}^{4M}$ and $\mathcal{U}_{j,M} \in \mathbb{R}^{3M}$, similarly as it was done with $\Psi_j \in \mathbb{R}^{4N}$ and $\mathcal{U}_j \in \mathbb{R}^{3N}$ in Section 4.3. The variable M denotes number of the transition points employed in the sparse planning horizon, while N is number of transition points in the short control horizon, which was used also in the trajectory following algorithm described in Section 4.3. Also values $\Delta t(k)$, $k \in \{N+1, \ldots, N+M\}$, that become variables in the planning horizon need to be gathered into vector $\mathcal{T}^{\Delta}_{j,M}$. All variables describing the complete trajectory (with both control and planning horizons) from the actual position of the separated sub-formation until the desired position within the original formation can be collected into the optimization vector $\Omega_{j,2} = [\Psi_j, \mathcal{U}_j, \Psi_{j,M}, \mathcal{U}_{j,M}, \mathcal{T}^{\Delta}_{j,M}] \in \mathbb{R}^{7N+8M}$.

The fault-recovery mechanism can be realized through the minimization of cost function $J_{j,2}(\Omega_{j,2})$ subject to equality constraints $h_j(k) = 0$, $\forall k \in \{0, \ldots, N+M-1\}$, $g_S(\psi_j(N+M)) = 0$ and inequality constraints $g_j(k) \leq 0, \forall k \in \{1, \ldots, N\}$. The stability constraint $g_S(\psi_j(N+M))$ guarantees that the found trajectory for the formation will reach its desired position DP. The stability constraint is given by $g_S(\psi_j(N+M)) := \|\bar{p}_j(N+M) - DP\|$, where $\bar{p}_j(N+M)$ is position of the last transition point in the trajectory. The constraints $h_j(\cdot)$ and $g_j(\cdot)$ are described in Section 4.3.

The cost function $J_{j,2}(\Omega_{j,2})$, employed in the trajectory planning and obstacle avoidance problem, is equivalent to the cost function $J_j(\Omega_j)$ from Eq. 3 except the first term penalizing deviation from the desired states. Here, this term is replaced by summation $\sum_{k=N+1}^{N+M} \Delta t(k)$, which minimizes the total time to reach the desired location DP. The value of the sum correlates with the estimated time of the formation movement in the planning horizon if the target would be static. In case of the formation re-coupling, even a moving main formation (and so moving DP) can be reached by the unstuck robots due to the periodical MPC replanning.

6 Experimental Results

Results presented in this section have been obtained by the proposed algorithm with the Sequential Quadratic Programming (SQP) method [38] employed for solving the optimization problems

used in the virtual leader trajectory tracking and for the stabilization and obstacle avoidance of followers. This solver provided the best performance from the tested available algorithms. Nevertheless, one can use any optimization method, which is able to solve the optimization problems defined in this paper.

6.1 Simulation of the Formation Movement with Obstacle Avoidance Tasks

The performance of the presented method in an environment with static and dynamic obstacles is shown in the simulation in Fig. 6. The method is used with parameters: $n=2$, $N=8$ and $\Delta t=0.25$ s.

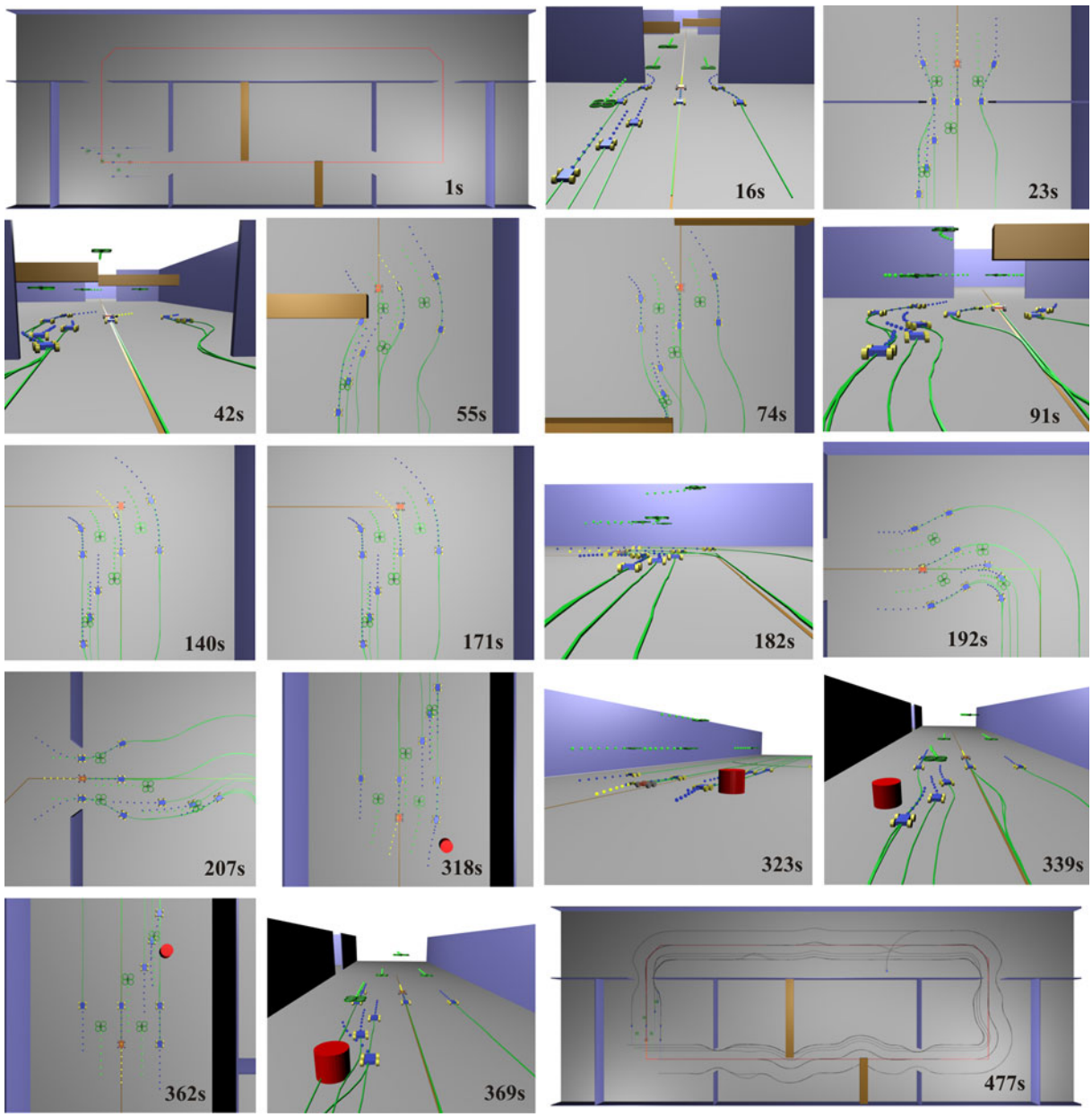

Fig. 6 Snapshots of the formation movement simulation

Table 1 Curvilinear coordinates of followers within the formation used in the experiment presented in Figs. 6 and 7

i	1	2	3	4	5	6	7	8	9	10	11	12
p_i	0	0	1	1	1	2	2.7	3.4	.5	.5	2.7	1.6
q_i	1	−1	1	−1	0	.6	.8	1	.5	−.5	.8	.2
h_i	0	0	0	0	0	0	0	0	.5	.5	.5	1

The experiment presents performance of this approach in scenarios inspired by a real world mission. The formation driving technique is employed in a surveillance application, in which a heterogeneous team of MAVs and UGVs has to periodically move through three rooms connected by a corridor. The objective of the mission is to follow a given path and to keep a desired shape of the

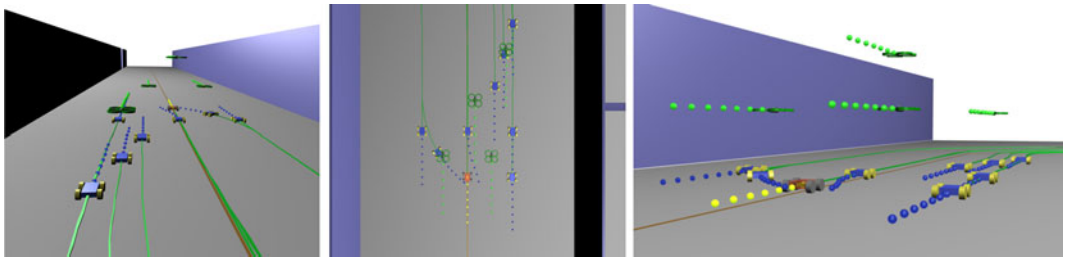

(a) Failure of follower 2 deviating from its desired position. 289s

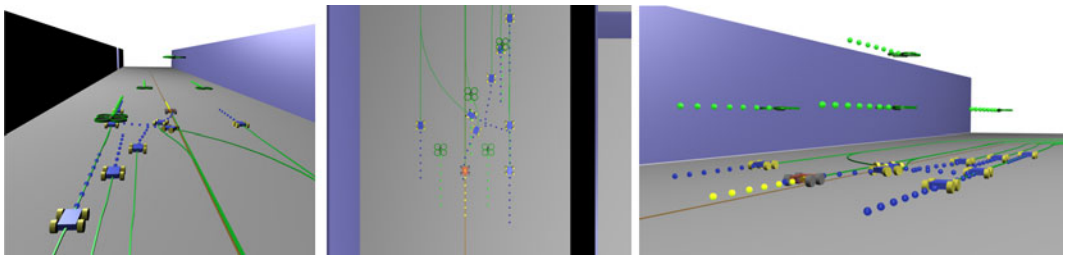

(b) Follower 5 avoiding the broken robot. 298s

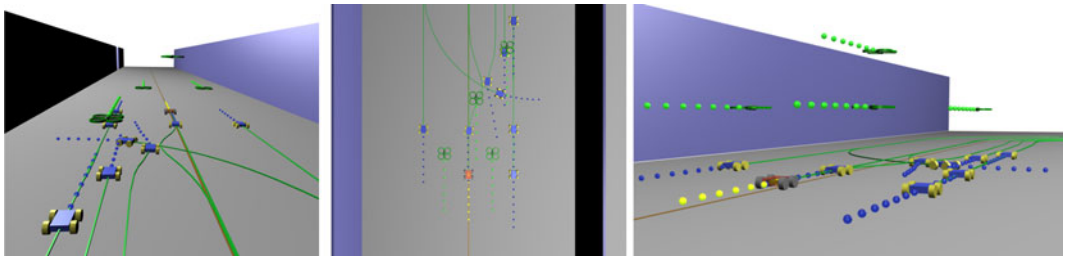

(c) Follower 6 avoiding the broken robot. 303s

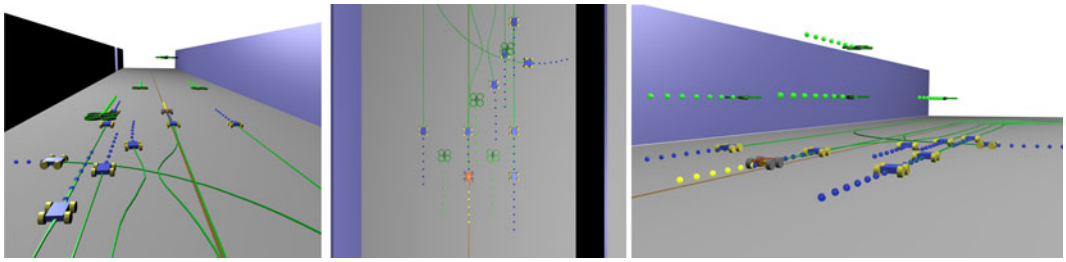

(d) All followers successfully avoided the broken robot. 308s

Fig. 7 Simulation of a response of the formation driving algorithm to a failure of one of the followers. The manoeuvre was recorded by three virtual cameras

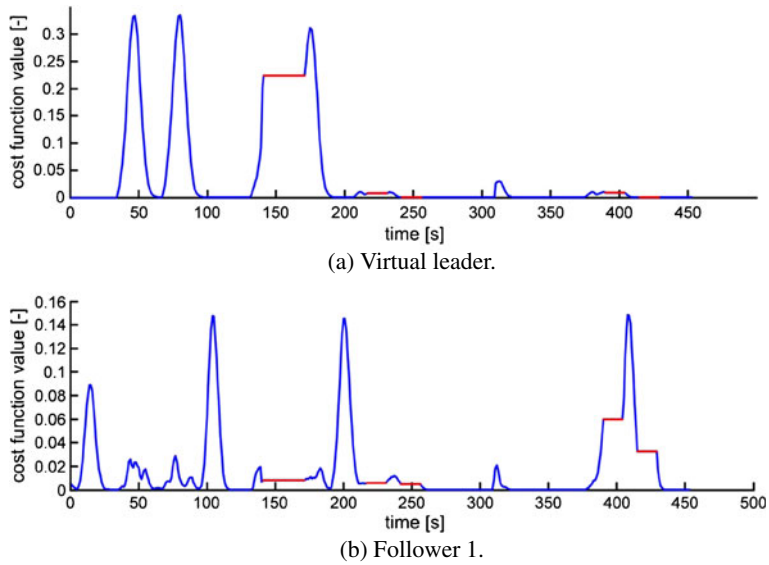

(a) Virtual leader.

(b) Follower 1.

Fig. 8 Progress of the cost function employed in the trajectory planning method during the movement presented in Figs. 6 and 7

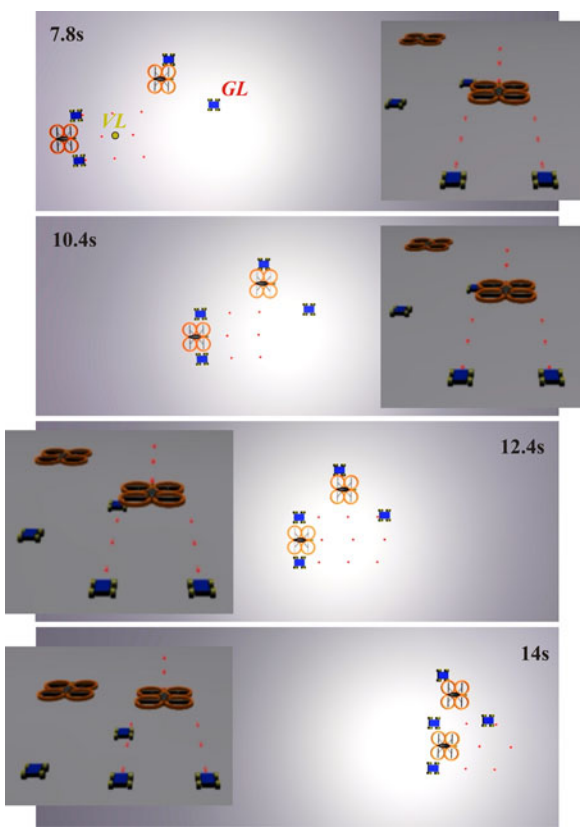

Fig. 9 MAVs-UGVs formation recovery after its undesired splitting into two independent units

formation. The formation can be autonomously temporarily shrunk in narrow passages (e.g. in doorways) or due to dynamic obstacles forcing followers to perform avoidance manoeuvres. The team (described in Fig. 2) consists of the GeNav leader (the orange robot denoted by GL), the virtual leader (the yellow robot denoted by VL), 8 UGV followers and 4 MAV followers. Three of the MAVs are positioned in a lower altitude to be able to relatively localize the ground robots. The fourth MAV is flying above them to provide relative positions of the lower MAVs. The MAV flying in the highest altitude could detect also the UGVs, but with much lower precision and reliability due to the greater relative distance and possibility of visibility interruption by one of the lower MAVs. Besides, the desired relative positions of the MAVs in the formation are determined in

Table 2 Performance of the fault-recovery mechanism with different ratio between the speed of the main formation ($v_{\text{main}} = 1$ in the experiments) and the speed of the unstuck formation v_{unstuck}

v_{unstuck}	1	1.1	1.2	1.3	1.4	1.5	1.6
Time	inf	41 s	21 s	14 s	10 s	8 s	7 s

The value of *Time* indicates time required for re-coupling of the sub-formation that was deviated from its desired position in distance 2 map units in x coordinate and 5 map units in y coordinate

such a way that they are not mutually influenced by air flow effects. The followers' coordinates relative to the virtual leader are presented in Table 1.

The initial position of the group is depicted in the first snapshot in Fig. 6 captured at time 1 s. In snapshots 16–23 s, the outer followers of the formation temporarily deviate from their desired positions to pass through the narrow passage towards the second room. The original shape of the formation is restored and the group starts avoiding the overhead obstacle in snapshots 42–55 s. The obstacle is sufficiently high to be passed under by all robots except the MAV flying in the highest altitude. The GeNav leader can be navigated without any influence of the obstacle, but the rest of the formation has to move away from the desired path to keep the constraints given by the relative localization. In the snapshot captured at time 55 s, one can see the deviation of the position of the virtual leader from the position of the GeNav leader. This enables to avoid the obstacle in a way that the obstacle is always situated outside the dilated convex hull of the formation. In the 74th second, the formation returns back on the desired path, but it is again forced to avoid the second overhead obstacle (snapshot at time 91 s). At time 140 s, the GeNav leader is approaching into the first connections of line segments of the path. The virtual leader and the followers are waiting for the GeNav leader, which has to turn on the spot. They are already deviated from the path to be able to smoothly continue without any complicated manoeuvring. Once the turning of the GeNav leader is finished (171 s), the complete formation continues back on the desired path (182 s, 192 s). At time 318 s, an unknown obstacle is detected by the formation. The obstacle is avoided, using the virtual leader's obstacle avoidance function, at the price of temporarily leaving of the desired path (snapshots at 323 s and 339 s). The second obstacle is detected by the followers, see snapshot at time 362 s. This dynamic obstacle cannot be avoided by the virtual leader's re-planning, since it was detected too late. Therefore, the avoidance function included in the follower's trajectory following method is utilized here. The shape of the formation is temporarily changed to keep the obstacle outside the dilated convex hull (369 s).

Cost-function values of the virtual leader's and the 1st follower's trajectory planning during the movement presented in Fig. 6 are depicted in Fig. 8. The peaks in the course of the leader's cost values correspond with the places of connections of line segments forming the desired path that has to be followed. In these connections, the virtual leader is forced to deviate from the path to be able to pass the sharp edges of the path smoothly.

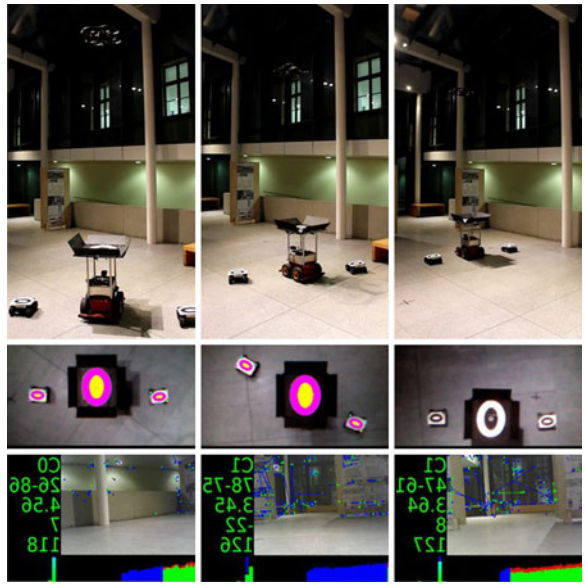

(a) Formation going through a connection of straight segments of the path.

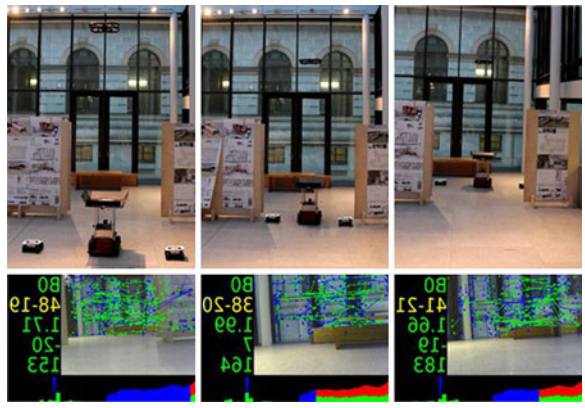

(b) Formation is temporarily shrinking to get through the narrow passage.

Fig. 10 Formation driving using the GeNav algorithm for the navigation and the top-view relative localization for the stabilization

Also the first unknown obstacle is contributing into the virtual leader's cost values. The temporal increase of cost values of the trajectory tracking of follower 1, which was chosen as an interesting example, is caused by the proximity of the obstacles. The obstacles force the robot to leave the desired position in the formation. The deviation from the desired state is penalized by the first term in the Eq. 3. The red lines in the courses of the values denote parts, in which the GeNav leader is turning to be able to follow the next path segment and the rest of the formation is waiting in static positions.

6.2 Simulations of the Fault Tolerance and Recovery

Beside the obstacle avoidance abilities, we have tested also the proposed fault-tolerant mechanism included in the formation driving scheme. As a part of the complex experiment presented in Fig. 6, a failure of one of the followers (its steering was blocked) has been simulated. The response of the formation to the undesired motion of the broken follower is in details shown in Fig. 7. In the snapshots, a successful avoidance manoeuvre of followers 5 and 6 as a response to prediction of the collision is demonstrated (see the last part of Eq. 3 for details on the applied avoidance function).

The second simulation (Fig. 9), verifying the proposed fault-recovery technique, presents the re-coupling of an inadvertently disconnected formation using the trajectory planning approach introduced in Section 5.2. In the experiment, the formation led by the robot equipped with the GeNav system (denoted as GL in the picture) follows a straight path segment. A sub-formation of two UGVs and one MAV has been separated from the group. In this unstuck group, a new virtual leader with position denoted as VL in the picture is created. Physically, the planning procedure of VL is run on a robot with sufficient computational power. It can be any robot from the original group, since it is assumed that the range of the visual relative localization (which cannot be interrupted) is significantly lower that the range of WiFi used for transfer of the plans for particular followers. The new formation starts its movement to reach the rest of the group from a location, which is deviated 2 map units sideways and 5 map units behind its desired position. As expected, the performance of the algorithm varies depending on the difference between the speed of the former formation and the maximal allowed speed of the unstuck group. This relation is shown in Table 2, where the performance of the formation recovery is expressed as the time needed for the re-coupling. It is obvious that in the case of same maximal allowed speed of both formations (the first column of the table), the unstuck formation cannot reach its desired position DP (denoted by the inf sign in the table).

a) b) c) d) e) f)

Fig. 11 Demonstration of the mechanism providing fault-tolerance in the MAVs-UGVs formation driving

6.3 Hardware Experiments

The experiment in Fig. 10a demonstrates the ability of the obstacle avoidance by temporary shrinking of the formation and it verifies the formation movement in a connection of path segments (Fig. 10b). In the experiment, the Pioneer 3-AT robotic platform is employed as the GeNav leader and two MMP5 platforms and the Ar.Drone MAV act as followers. Beside the pictures of the formation movement, images used for the GeNav visual navigation and for the top-view relative localization are shown in Fig. 10 and in a video record of the experiment [39].

In the final experiment, the failure recovery mechanism is shown in practice (see Fig. 11). The employed formation consists of a G2Bot-Testbed of the Czech Technical University employed as the leader and the MMP5 robot and the Ar.Drone used as followers. In the experiment, the MMP5 follower is firstly slightly pushed from its position within the formation, which is corrected based on the information from the top view relative localization only. The failure of the formation integrity is demonstrated by the forced shift of the robot behind the formation, which is again compensated to achieve the desired shape of the formation.

7 Conclusion

In this paper, a novel fault-tolerant formation driving approach developed for heterogeneous MAVs-UGVs teams was proposed. The core of the method consists in stabilization of the compact 3D formation by the top-view visual relative localization in control feedback. Besides, the proposed method is suited for utilization of a simple visual navigation of the formation based on detection of features in images obtained by an onboard camera. It was shown that these simple on-board vision based systems enable to deploy teams of closely cooperating unmanned ground and aerial vehicles in environments without any pre-installed infrastructure for robots' localization. Beyond the description and experimental verification of the proposed method, the fault diagnosis and recovery mechanisms were provided in the paper.

Acknowledgement This work was supported by GAČR under M. Saska's postdoc grant no. P10312/P756.

References

1. Faigl, J., Krajník, T., Chudoba, J., Preucil, L., Saska, M.: Low-cost embedded system for relative localization in robotic swarms. In: Proc. of IEEE International Conference on Robotics and Automation (2013)
2. Krajník, T., Faigl, J., Vonásek, M., Kulich, V., Košnar, K., Přeučil, L.: Simple yet stable bearing-only navigation. J. Field Robot. **27**(5), 511–533 (2010)
3. Saska, M., Krajník, T., Přeučil, L.: Cooperative micro uav-ugv autonomous indoor surveillance. In: IEEE SSD (2012)
4. Dong, W.: Robust formation control of multiple wheeled mobile robots. J. Intell. Robot. Syst. **62**(3–4), 547–565 (2011)
5. Hengster-Movrić, K., Bogdan, S., Draganjac, I.: Multi-agent formation control based on bell-shaped potential functions. J. Intell. Robot. Syst. **58**(2), 165–189 (2010)
6. Liu, Y., Jia, Y.: An iterative learning approach to formation control of multi-agent systems. Syst. Control Lett. **61**(1), 148–154 (2012)
7. Do, K.D., Lau, M.W.: Practical formation control of multiple unicycle-type mobile robots with limited sensing ranges. J. Intell. Robot. Syst. **64**(2), 245–275 (2011)
8. Ghommam, J., Mehrjerdi, H., Saad, M., Mnif, F.: Formation path following control of unicycle-type mobile robots. Robot. Auton. Syst. **58**(5), 727–736 (2010)
9. Sira-Ramiandrez, H., Castro-Linares, R.: Trajectory tracking for non-holonomic cars: a linear approach to controlled leader-follower formation. In: IEEE Conf. on Decision and Control (CDC) (2010)
10. Xiao, F., Wang, L., Chen, J., Gao, Y.: Finite-time formation control for multi-agent systems. Automatica **45**(11), 2605–2611 (2009)
11. No, T.S., Kim, Y., Tahk, M.-J., Jeon, G.-E.: Cascade-type guidance law design for multiple-uav formation keeping. Aerosp. Sci. Technol. **15**(6), 431–439 (2011)
12. Saffarian, M., Fahimi, F.: Non-iterative nonlinear model predictive approach applied to the control of helicopters group formation. Robot. Auton. Syst. **57**(67), 749–757 (2009)
13. Liu, C., Chen, W.-H., Andrews, J.: Piecewise constant model predictive control for autonomous helicopters. Robot. Auton. Syst. **59**(78), 571–579 (2011)
14. Abdessameud, A., Tayebi, A.: Formation control of vtol unmanned aerial vehicles with communication delays. Automatica **47**(11), 2383–2394 (2011)
15. Tanner, H., Christodoulakis, D.: Decentralized cooperative control of heterogeneous vehicle groups. Robot. Auton. Syst. **55**(11), 811–823 (2007)
16. Isermann, R.: Fault-Diagnosis Systems: An Introduction from Fault Detection to Fault Tolerance. Springer (2006)
17. Freddi, A., Longhi, S., Monteriu, A.: Actuator fault detection system for a mini-quadrotor. In: IEEE Inter-

national Symposium on Industrial Electronics (ISIE), pp. 2055–2060. IEEE (2010)
18. Heredia, G., Ollero, A., Bejar, M., Mahtani, R.: Sensor and actuator fault detection in small autonomous helicopters. Mechatronics **18**(2), 90–99 (2008)
19. Ranjbaran, M., Khorasani, K.: Fault recovery of an under-actuated quadrotor aerial vehicle. In: 49th IEEE Conference on Decision and Control (CDC), pp. 4385–4392. IEEE (2010)
20. Ranjbaran, M., Khorasani, K.: Generalized fault recovery of an under-actuated quadrotor aerial vehicle. In: American Control Conference (ACC), pp. 2515–2520. IEEE (2012)
21. Mead, R., Long, R., Weinberg, J.B.: Fault-tolerant formations of mobile robots. In: IEEE/RSJ IROS, pp. 4805–4810. IEEE (2009)
22. Chamseddine, A., Zhang, Y., Rabbath, C.A.: Trajectory planning and re-planning for fault tolerant formation flight control of quadrotor unmanned aerial vehicles. In: American Control Conference (ACC), pp. 3291–3296. IEEE (2012)
23. Heredia, G., Caballero, F., Maza, I., Merino, L., Viguria, A., Ollero, A.: Multi-uav cooperative fault detection employing vision based relative position estimation. In: Proceedings of the 17th IFAC World Congress, pp. 12 093–12 098 (2008)
24. Heredia, G., Caballero, F., Maza, I., Merino, L., Viguria, A., Ollero, A.: Multi-unmanned aerial vehicle (UAV) cooperative fault detection employing differential global positioning (DGPS), inertial and vision sensors. Sensors **9**(9), 7566–7579 (2009)
25. Ismail, A.R., Timmis, J.: Aggregation of swarms for fault tolerance in swarm robotics using an immunoengineering approach. In: UK Workshop on Computational Intelligence (2009)
26. Christensen, A.L., O'Grady, R., Dorigo, M.: From fireflies to fault-tolerant swarms of robots. IEEE Trans. Evol. Comput. **13**(4), 754–766 (2009)
27. Barambones, O., Etxebarria, V.: Robust adaptive control for robot manipulators with unmodelled dynamics. Cybern. Syst. **31**(1), 67–86 (2000)
28. Alamir, M.: Stabilization of Nonlinear Systems Using Receding-Horizon Control Schemes. Ser. Lecture Notes in Control and Information Sciences, vol. 339. Springer, Berlin/Heidelberg (2006)
29. Mayne, D.Q., Rawlings, J.B., Rao, C.V., Scokaert, P.O.M.: Constrained model predictive control: stability and optimality. Automatica **36**(6), 789–814 (2000)
30. Boscariol, P., Gasparetto, A., Zanotto, V.: Model predictive control of a flexible links mechanism. J. Intell. Robot. Syst. **58**(2), 125–147 (2010)
31. Chao, Z., Zhou, S.-L., Ming, L., Zhang, W.-G.: Uav formation flight based on nonlinear model predictive control. Math. Probl. Eng. **2012**(1), 1–16 (2012)
32. Defoort, M.: Distributed receding horizon planning for multi-robot systems. In: IEEE International Conference on Control Applications (CCA), pp. 1263–1268 (2010)
33. Zhang, X., Duan, H., Yu, Y.: Receding horizon control for multi-uavs close formation control based on differential evolution. Sci. China Inf. Sci. **53**(2), 223–235 (2010)
34. Saska, M., Krajník, T., Vonásek, V., Vanek, P., Preucil, L.: Navigation, localization and stabilization of formations of unmanned aerial and ground vehicles. In: ICUAS (2013)
35. Krajník, T., Nitsche, M., Pedre, S., Přeučil, L., Mejail, M.: A simple visual navigation system for an UAV. In: International Multi-Conference on Systems, Signals and Devices, p. 34. IEEE, Piscataway (2012)
36. Krajník, T., Vonásek, V., Fišer, D., Faigl, J.: AR-drone as a platform for robotic research and education. In: Research and Education in Robotics: EUROBOT 2011. Springer, Heidelberg (2011)
37. Barfoot, T.D., Clark, C.M.: Motion planning for formations of mobile robots. Robot. Auton. Syst. **46**, 65–78 (2004)
38. Nocedal, J., Wright, S.J.: Numerical Optimization. Springer (2006)
39. Movie: Movie of hw experiment and simulation presented in this paper. Online: http://imr.felk.cvut.cz/formation/ (2013). cit. 2013-2-22